

The Jungle of Generative Drug Discovery: Traps, Treasures, and Ways Out

Rıza Özçelik^{1,2} Francesca Grisoni*^{1,2}

Abstract

“How to evaluate de novo designs proposed by a generative model?” Despite the transformative potential of generative deep learning in drug discovery, this seemingly simple question has no clear answer. The absence of standardized guidelines challenges both the benchmarking of generative approaches and the selection of molecules for prospective studies. In this work, we take a fresh – *critical* and *constructive* – perspective on de novo design evaluation. We systematically investigate widely used evaluation metrics and expose key pitfalls (‘traps’) that were previously overlooked. In addition, we identify tools (‘treasures’) and strategies (‘ways out’) to navigate the complex ‘jungle’ of generative drug discovery, and strengthen the connections between the molecular and deep learning fields along the way. Our systematic and large-scale results are expected to provide a new lens for evaluating the de novo designs proposed by generative deep learning approaches.

Discovering new therapeutics is an adventure as old as human civilization. However, finding new drug molecules is more resource-intensive today than ever^[1,2]. A key challenge lies in the vastness of the ‘chemical universe’ – estimated to contain more than 10^{60} drug-like molecules – where compounds with desirable biological properties are exceedingly rare^[3]. Artificial intelligence (AI) has emerged as a transformative technology for drug discovery, to help find the ‘needle in the haystack’. By supporting virtual screening^[4–6] and de novo molecule design^[7–12], AI can narrow down the chemical universe, and it is nowadays widely adopted in academia and industry^[13–17]. Generative deep learning has garnered particular attention for drug discovery. Powered by deep neural networks, these models can learn how to generate molecules with desired properties on-demand, and have already demonstrated success in

prospective studies^[7,18–21].

Generative drug discovery generally involves three stages: *train*, *generate*, and *evaluate*. After almost a decade from its initial introduction^[22,23], prolific research has standardized many aspects of model *training*^[13–15,24–26] and molecule *generation*^[9,24,26,27]. However, the third stage – *evaluation* – remains relatively underinvestigated, with choices left to the single practitioners. The *evaluation* of molecular designs (e.g., in terms of their overall quality, relevance, and ultimately, ranking) holds a crucial role. First, selecting the best candidates from thousands of designs determines the success or failure of follow-up experiments. Second, robust evaluation of the generated molecules is essential to monitor progress in the field, and to compare different approaches. Yes, despite notable efforts to standardize model evaluation^[28–31], no consensus within the community has been reached^[24,32–34].

Here, we dive into design evaluation, with a *critical* and *constructive* perspective. We conduct a systematic study evaluating around 10^9 de novo designs across three state-of-the-art deep learning architectures. Our results uncover a previously overlooked pitfall: the size of a design library can systematically bias the evaluation, and at times even falsify the scientific findings by overshadowing molecular quality. We then draw new connections between drug discovery and deep learning to facilitate molecule selection for prospective studies. Finally, we leverage the tools we develop to dig deeper into the *generation* stage, and expose unique characteristics of molecule design, compared to other applications of deep learning.

To capture the complexity on the landscape of generative drug discovery, we introduce the analogy of a ‘jungle’, where we identify criticalities (‘traps’), useful tools (‘treasures’), and guidelines (‘ways out’). These findings aim to redefine how generative models are evaluated in drug discovery and provide a roadmap for selecting molecules with higher confidence for real-world applications.

Results and discussion

While many approaches exist to design molecules de novo, ‘chemical language’ models (CLMs) have been among the most successful^[25,35,36]. CLMs are trained to generate

¹Institute for Complex Molecular Systems and Dept. Biomedical Engineering, Eindhoven University of Technology, Eindhoven, The Netherlands. ²Centre for Living Technologies, Alliance TU/e, WUR, UU, UMC Utrecht, The Netherlands. Correspondence to: Francesca Grisoni <f.grisoni@tue.nl>.

molecules in the form of molecular strings, such as Simplified Molecular Input Line Entry Systems (SMILES)^[37] and Self-referencing embedded strings (SELFIES)^[38]. Since CLMs can be trained and used to generate molecules in a time-efficient manner^[26], and excel at capturing complex molecular properties^[36], they constitute an ideal choice for a large-scale analysis like ours.

Here, we use three deep CLM architectures: (i) Recurrent neural networks with long short-term memory cells, (LSTM)^[22,39], which learn from and generate chemical sequences one symbol ('token') at a time; (ii) Generative Pretrained Transformers (GPT)^[40,41], which, via the attention mechanism^[42] learn all pair relationships between input tokens; and (iii) Structured State-Space Sequence models (S4)^[26,43], which were recently introduced, and learn from entire sequence at once, while generating token-by-token. After pre-training the CLMs on 1.5M canonical SMILES strings from ChEMBLv33^[44], they were fine-tuned on bioactive molecules of three macromolecular targets^[45]: (a) Dopamine Receptor D3 (DRD3), (b) Peptidyl-prolyl cis/trans Isomerase NIMA-interacting 1 (PIN1), and Vitamine D Receptor (VDR). The fine-tuning was repeated five times for each target, with a different random set of 320 bioactive molecules each. From each fine-tuned CLM, we sampled 1,000,000 molecules in the form of SMILES strings (using multinomial sampling, equation (1)).

The size of de novo design libraries can fool you

"How many designs should I generate?" Every de novo design study faces this question. Although an arbitrary number of SMILES strings could be generated, 1000 and 10,000 designs are typical choices for model evaluation^[28]. However, since generative molecule design involves sampling from a learned probability distribution, a minimum library size may be required to ensure a representative overview of the model's output. Here, we aim to shed light on (a) what library size is sufficient to comprehensively evaluate the quality of designs, and (b) whether the number of chosen designs affects the evaluation outcomes. To this end, we evaluated the following aspects in increasing number of de novo designs:

- *Similarity between de novo designs and fine-tuning sets.* We measured the Frechét ChemNet Distance (FCD)^[46], which captures the biological and chemical similarity of two molecular sets (through the ChemNet^[47] model). Moreover, we computed the Frechét distance^[48] on five molecular descriptors (Frechét Descriptor Distance, FDD, *see* Methods). The lower the FDD, the closer the sets of molecules are in terms of the distribution of their physicochemical properties. As controls, we computed the FCD and FDD values of 128 held-out actives and 1280 inactives per each data

split, with the hypothesis that active molecules should be closer to the fine-tuning set than the inactive ones.

- *Internal diversity of designed libraries.* We calculated three metrics: (a) uniqueness, that is, the fraction of unique (and 'chemically' valid) canonical SMILES strings generated, (b) the number of clusters containing structurally distant molecules (related to '#Circles'^[32,49]), as identified via sphere exclusion algorithm^[32,49], and (c) number of unique substructures, identified via Morgan algorithm^[50]. To our knowledge, this is the first study that uses this latter metric to evaluate internal diversity.

These aspects were systematically evaluated by varying the size of the generated library of de novo designs, from 10^2 to 10^6 molecules.

Similarity. A relationship was observed between distribution similarity and the number of de novo designs considered (Fig. 1). FCD values decreased across all targets when increasing the library size (Fig. 1a), reaching a plateau. Such FCD plateau was systematically reached when more than 10,000 designs were considered – a higher number than what is usually considered in de novo design studies. Although the authors of FCD recommend using at least 5000 molecules in each set to be compared^[46], our analysis shows that FCD can also be used with smaller training set sizes typical of drug discovery campaigns, since FCD converges when enough designs are generated.

The FCD between inactive and fine-tuning molecules was, contrary to expectations, lower than that of the active molecules that were held-out for PIN1 and VDR (Fig. 1a). This is because the number of inactives is nine times greater than the number of actives. The design libraries reached FCD values lower than those of the held-out actives across proteins, again as an effect of the library size. These findings demonstrate the cruciality of comparing molecule libraries of the same size when using FCD.

Unlike FCD, FDD scores held-out actives as more similar to the training set than inactives, across targets and scales (Fig. 1b). However, FDD also decreases as the library size increases, revealing that it is also sensitive to the number of molecules used to compute the distance. This behavior highlights how reporting descriptor similarity in an arbitrary number of molecules can be misleading. Our findings underscore the library size, an overlooked parameter of the evaluation stage, as a key confounding factor of measured distributional distance between molecule libraries. We define this confounding effect here as the 'size trap'.

Internal Diversity. Uniqueness – commonly reported to compare generative approaches – decreases with increasing number of designs and can lead to ranking models differently depending on the considered number of designs

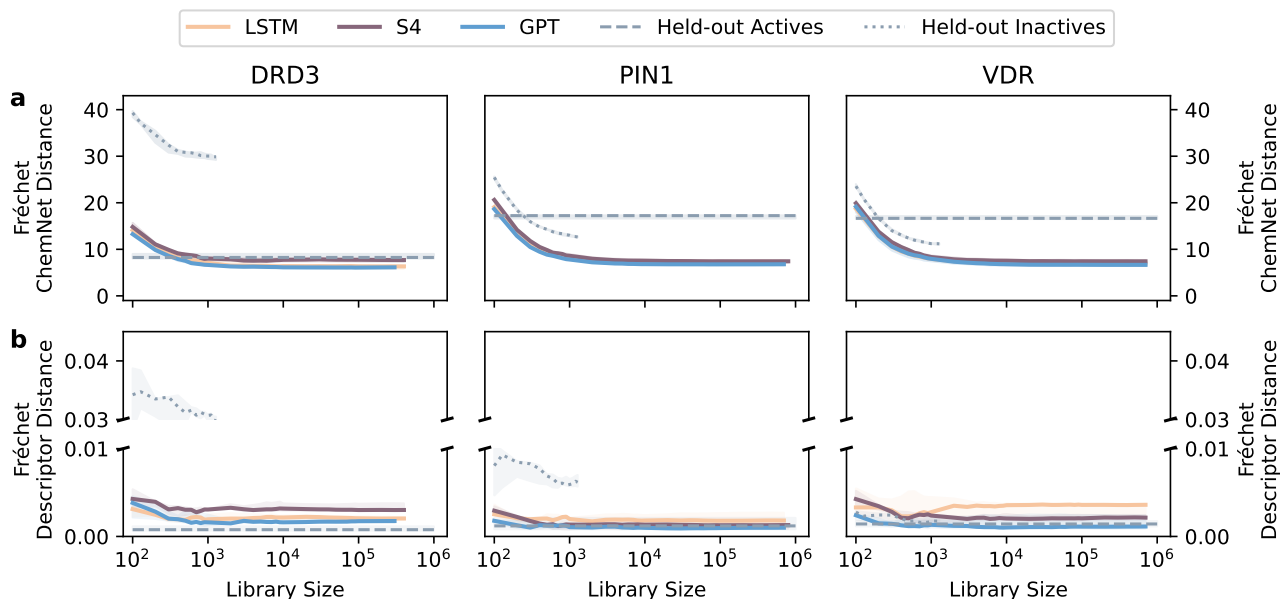


Figure 1. The size trap similarity to existing molecules. Fréchet ChemNet Distance (FCD, **a**) and Fréchet Descriptor Distance (FDD, **b**) are measured in increasing library sizes. Solid lines denote the median distance between design libraries and respective fine-tuning sets, across five repetitions ($n = 5$) and shaded regions display the first and third quartiles. Dashed lines display the median distance of held-out actives ($n = 128$) and inactives ($100 \leq n \leq 1280$), to the training sets.

(Fig. 2a). The number of clusters also depends on the size of the library, with performance differences becoming progressively more pronounced for larger libraries (Fig. 2b). Unlike uniqueness, the models’ relative performance remains consistent across scales when the number of clusters is considered. Thus, we view uniqueness as a ‘sanity check’ for mode collapse, rather than a reliable diversity metric. Finally, the number of substructures shows the same trend as the number of clusters (Pearson correlation coefficient larger than 99% across experiments), even when these scores are divided by the library size (Fig. S1), and when non-synthesizable designs were filtered out before computation (Fig. S2). Finally, the number of substructures is up to 85 times faster to compute (Fig. S3), making it a recommended alternative to computing the number of clusters.

Navigating large design libraries with likelihoods

The observed ‘size trap’ makes it necessary to analyze large design libraries for robust evaluation. However, this comes with an increased overhead when ranking and selecting molecules from large libraries (e.g., for follow-up prospective studies). Often, criteria based on subjective judgment/expertise are used, which makes the analysis prone to bias and limits its broader applicability. Here, we explore the model likelihoods – which capture how well a

SMILES sequence aligns with the information learned by the model during training (equation (2)) – as a strategy for library rationalization. Likelihoods can be computed for any design and for the majority of the popular deep generative models^[39,51,52]. Albeit likelihoods have already been introduced for de novo design^[26,53,54], an open question remains as to how they can be used systematically navigate large design libraries.

Here, after generating 1,000,000 designs from a fine-tuned model (LSTM in this selected example), we computed the designs’ likelihoods and binned them into deciles of increasing likelihood. We inspected the designs of each decile for: (i) syntactic score, i.e., the fraction of chemically valid SMILES strings (validity) and molecules not in the training sets (novelty); (ii) structural similarity to the fine-tuning set, computed as maximum Tanimoto similarity on extended connectivity fingerprints^[50] of novel and unique designs; and (iii) number of substructures, to capture the internal diversity of each decile.

The likelihood deciles reveal an exploration-exploitation trade-off. Higher likelihood bins show higher validity and structural similarity to active molecules (exploitation) (Fig. 3a,b), but contain fewer novel molecules and substructures (Fig. 3a,c). In contrast, decreasing likelihoods favor exploration (generating novel molecules and substructures) at the cost of similarity to known bioactives and

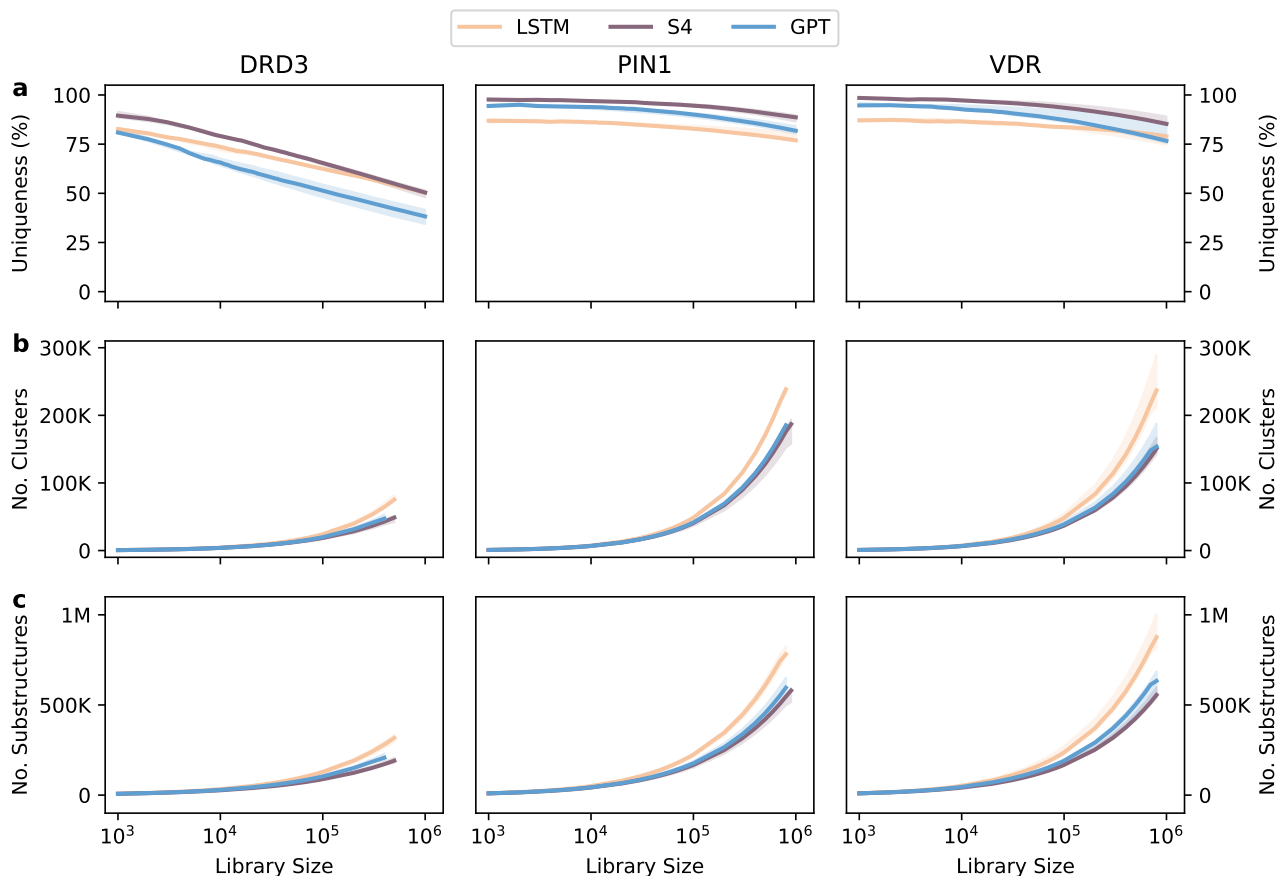


Figure 2. The size trap - internal diversity. Three internal diversity metrics are measured in increasing library sizes. **(a)** Uniqueness, that is the fraction of distinct designs among the chemically-valid ones. **(b)** Number of clusters, computed via sphere exclusion clustering, denotes the number of structurally distant molecules in the library. **(c)** Number of substructures, i.e., number of unique Morgan keys^[50]. For all figures, lines display the median score measured across five fine-tuning repetitions ($n=5$) and the shaded regions show the first and third quartiles.

validity. These trends are consistent across model architectures (Fig. S4, S5) and targets.

For a selected fine-tuned model (LSTM) and target (DRD3), we analyzed the most frequently occurring generic scaffolds^[55] of the designs across likelihood deciles (1st, 4th, 7th, and 10th). These scaffold were compared to the respective fine-tuning set (Fig. 4). Higher likelihood bins featured frequent scaffolds identical or similar to those of active molecules, while lower bins contain simpler, repeated scaffolds, such as single or fused rings (Fig. 4a). These observations show how likelihood (and the corresponding exploration-exploitation trade-off) can be tuned based on the envisioned application, e.g., chemical space navigation (exploration) vs hit-to-lead optimization (exploitation).

Finally, when analyzing the frequently occurring (generated more than ten times) molecular structures, we found

that frequent design can have low quality, consisting only of simple substructures (e.g., benzene, amine, and ether groups), making them unsuitable for prospective studies (Fig. 4b). These low-quality designs, similar to ‘recurring hallucinations’ in language models^[56], appear in the least likely decile, despite being frequently generated (Fig. S6). This ‘count trap’ underscores the need to integrate likelihoods into frequency-based evaluations to avoid overemphasizing such designs.

Ultimately, our analysis shows that model likelihood is a cost-efficient and model-intrinsic score not only to navigate the exploration-exploitation trade-off for prospective studies, but also to identify and mitigate low quality, repetitive generations, such as recurring hallucinations.

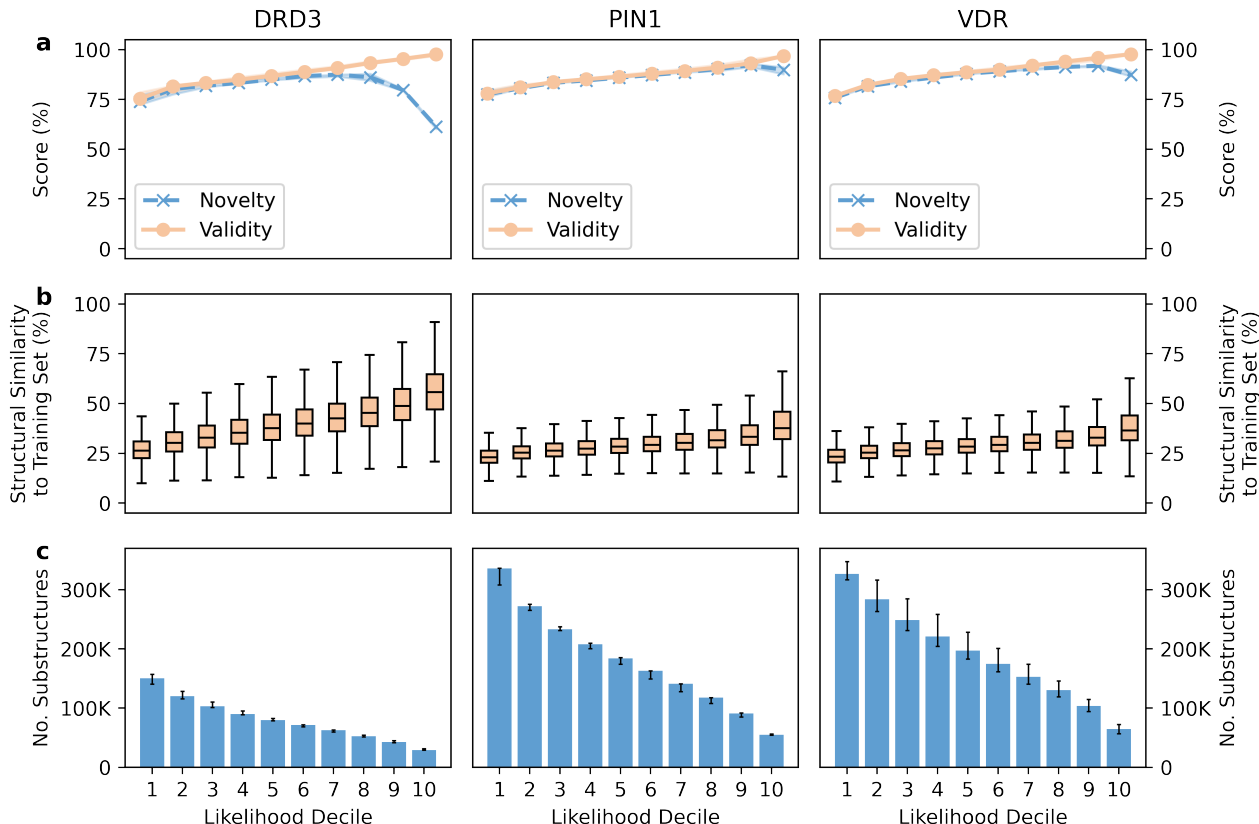


Figure 3. Navigating large design libraries. We bin the designs per protein target into ten increasing likelihood bins and compute metrics for the designs in each decile. **(a)** Fraction of valid (validity) and unique molecules not in the respective training set (novelty) are computed. The lines represent the median across five fine-tuning campaigns and the shaded regions mark the first and third quartiles. **(b)** Structural similarity of the designs to the training set per decile is computed via Tanimoto similarity over extended connectivity fingerprints^[50]. Similarities are pooled across five repetitions and visualized as a box plot. **(c)** The diversity in each decile is computed via the number of substructures. Bar heights denote the median across runs while the error bars mark the first and third quartiles.

The curious case of molecule generation with deep learning

Another key step in generative drug discovery is the generation of molecule itself, which involves sampling from the probability distributions learned by the model. Temperature sampling – based on weighted random sampling of tokens (equation (1)) – is the most common sampling approach to date for de novo design^[28,29]. However, when looking at the field of natural language processing, two other strategies have shown better performance^[57,58]: (a) top- k sampling^[58,59], which considers only the most likely k tokens at each generation step, and (b) top- p sampling^[57], which uses only a token subset, covering more than $p\%$ of the probability distribution. Although these strategies outperform temperature sampling in natural language processing, they have found limited application in the molecular domain^[9].

Using the fine-tuned LSTM models, we used each sampling strategy to generate 1,000,000 designs, using different values of temperature T ($0.5 \leq T \leq 2$), k ($3 \leq k \leq 33$), and p ($0.5 \leq p \leq 1$). Increasing T , k , and p increases the randomness of sampling (*see Methods*). We measured validity, novelty, structural similarity to the fine-tuning set, and number of substructures.

Temperature has the greatest impact on the characteristics of de novo designs (Fig. 5). Higher temperature values increase the design diversity across datasets (Fig. 5a,c), but reduce validity and similarity to the fine-tuning set (Fig. 5a,b), in agreement with previous works^[9,26]. For top- k sampling, The smallest value of k ($k = 3$) causes mode collapse, i.e., designs are valid but repetitive (Fig. 5a), suggesting that considering three candidate tokens might be insufficient to design diverse molecules. For $k \geq 5$, the sampling behavior approximates temperature sampling

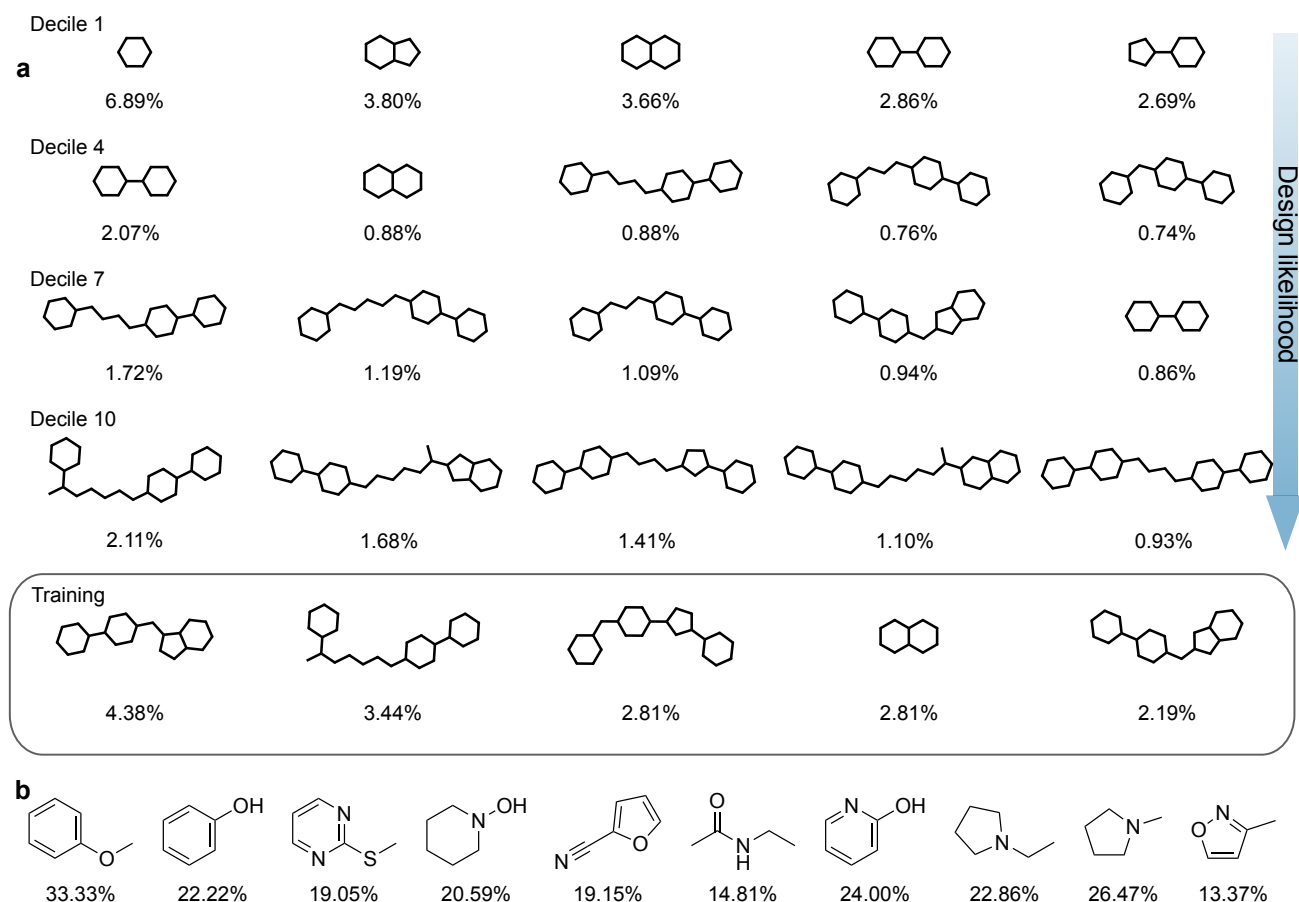


Figure 4. Likelihoods and exploration-exploitation trade-off. Designs of LSTM trained on a DRD3 dataset are binned into increasing likelihood deciles. **(a)** The most repeating generic Bemis-Murcko scaffold from deciles, 1, 4, 7, and 10 are visualized, as well as the training set. The number below each scaffold denotes their frequency in the library. **(b)** The least likely 10 designs that are sampled more than 10 times are retrieved and visualized. Maximum structural similarity to the fine-tuning sets are reported below the molecules.

with $T = 1$, indicating that the top-5 tokens already cover the most likely tokens. Top- p sampling behaves similarly to top- k sampling. For $p \leq 0.9$, designs are valid but repetitive, while larger values of p resemble temperature sampling ($T = 1$). In the former case, few tokens cover the p threshold, causing mode collapse; in the latter case, adding more tokens has little effect due to their low probability. We call this behavior, which is consistent across model architectures (Fig. S7, S8), ‘filtering trap’.

These findings contrast with natural language generation: while top- k and top- p outperform temperature sampling to generate natural language, temperature sampling is the primary sampling strategy to control molecule diversity. To gain further insights, we generated 102,400 designs (using the fine-tuned LSTM for VDR) and analyzed the frequency of appearance of each token in the top-5 and top-90% of the distribution (Fig. 6a,b), along with their mean sampling probability (Fig. 6c). While probable tokens,

such as carbon, are consistently likely across generation steps, most tokens rarely appear among the top-5 and top-90%. This skewed distribution differentiates molecule design from natural language generation, where tokens can be sampled among hundreds of thousands of candidates. In the molecular field, the number of tokens is inherently constrained due to the number of elements that can be used in drug-like molecules, leading to a higher concentration of likely candidates and a less diverse set of options at each generation step. Overall, our analysis reveals a unique behaviour of molecule generation, and exemplifies the gaps between natural language and drug discovery applications.

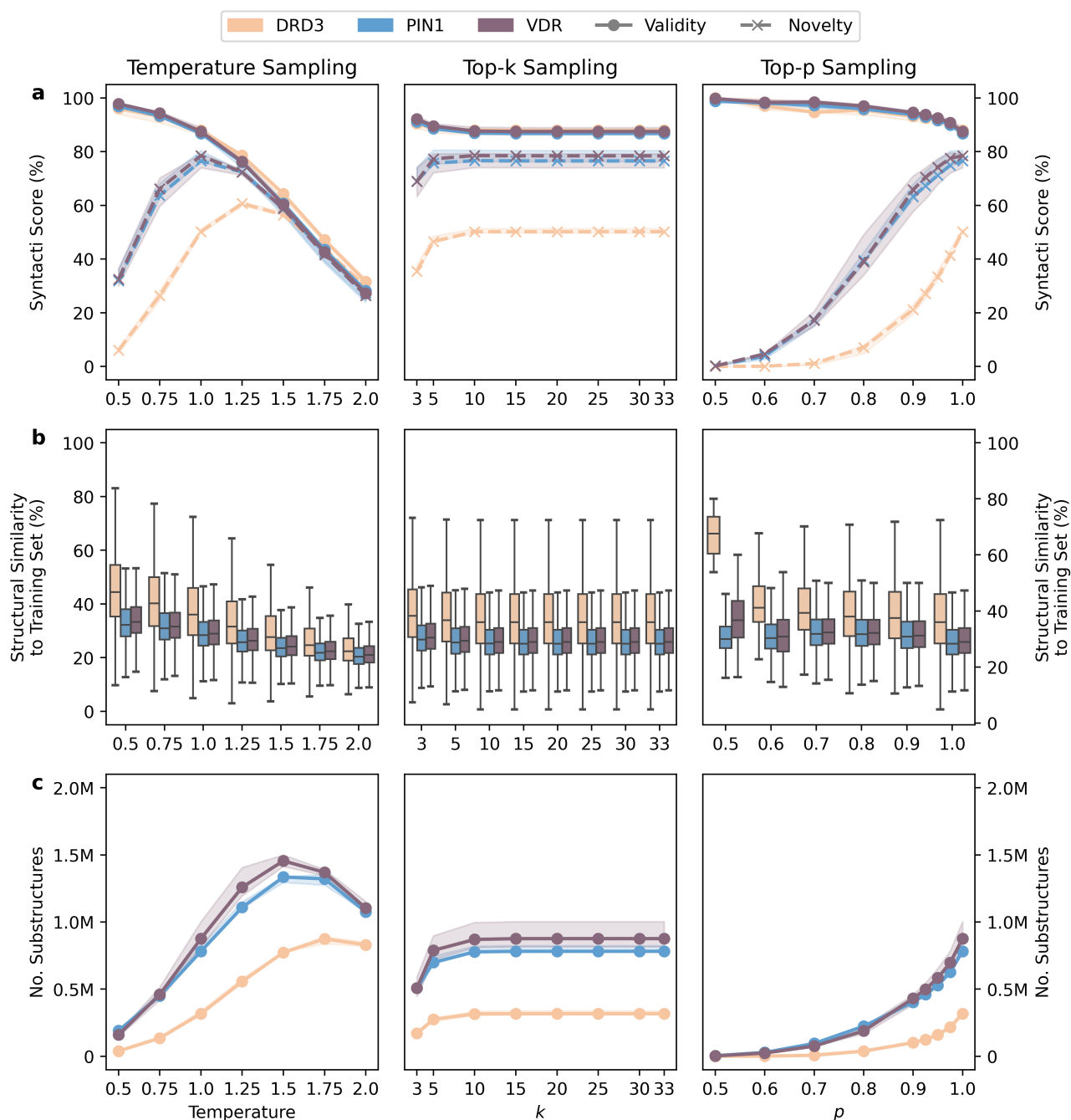


Figure 5. Benchmarking molecule sampling strategies. The fine-tuned LSTM models across datasets are sampled using temperature, top- k , and top- p sampling, in different temperature, k , and p values. 1,000,000 designs are produced per dataset split and sampling parameter combination. **(a)** Syntactic quality of the designs as measured by the fraction of valid (validity) and unique and novel compounds (novelty). The lines denote the median across five repetitions and the borders of the shaded areas display first and third quartiles. **(b)** Maximum structural similarity of each design to the respective training set is computed (as Tanimoto similarity on extended connectivity fingerprints^[50]) and the values across datasets splits are visualized as boxplots ($n \approx 5,000,000$). **(c)** Diversity of the designs are measured via the number of structures, i.e., the number of unique Morgan keys identified^[50]. The lines denote the median of five runs and the shaded regions denote the inter-quartile ranges.

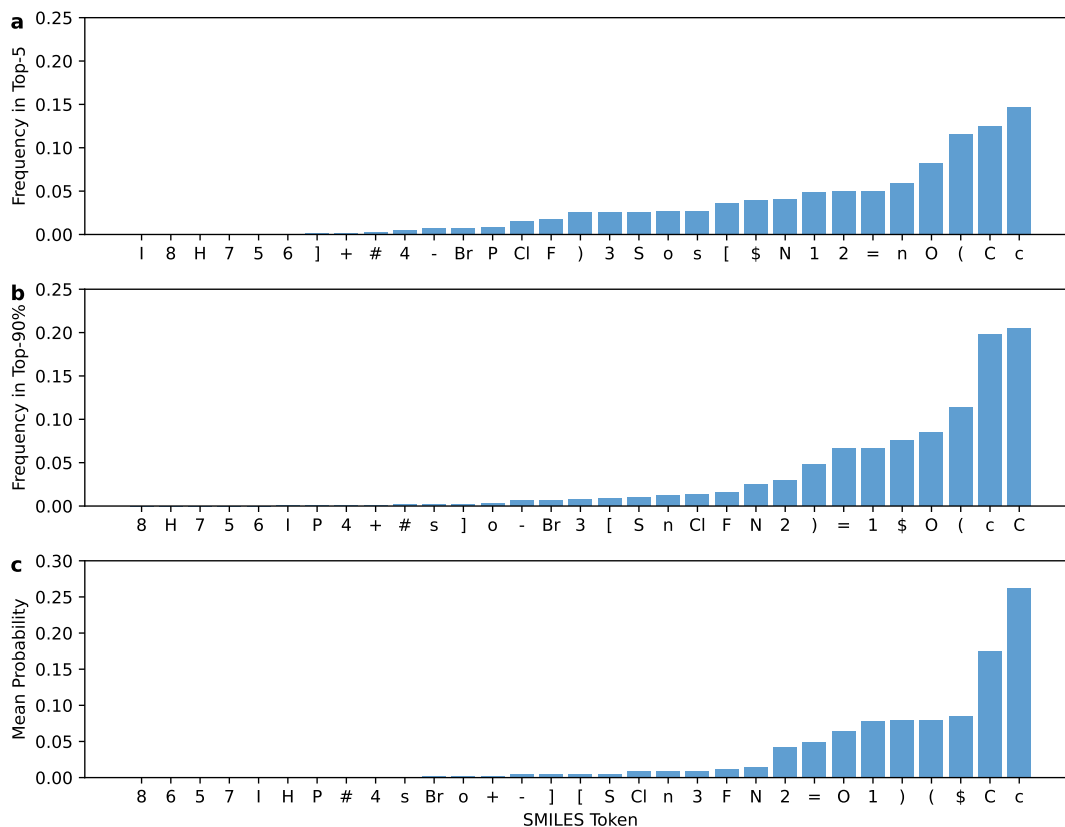


Figure 6. *The curious case of molecule sampling.* 102,400 designs are generated with an LSTM model fine tuned on VDR dataset. The frequency of appearing in (a) top-5, (b) top-90% of the distribution, and (c) mean sampling probability across generation steps is computed per SMILES token. Element symbols annotate the atom types in SMILES strings (lower-casing corresponds to aromaticity), whereas bonds are encoded with '=' (double bond) and '#' (triple bond) tokens^[37]. Opening and closing brackets denote branch beginning and ending, respectively, and digits define ring structures. Square brackets, '+', and '-' signs are used for explicit charge annotations. The '\$' symbol is used to denote the end of the SMILES string for this plot.

Orienteering in the jungle of generative drug discovery

Generative deep learning is reshaping computer-assisted drug discovery, and we have only begun to test its potential and boundaries. In this context, robust evaluation pipelines are essential to identify and eventually expand these boundaries. Thanks to our large-scale analysis, our work highlights previously overlooked challenges and untapped opportunities in the application of generative deep learning to drug discovery. These findings, in turn, highlight new solutions for evaluating generative drug discovery models (Table 1).

One of the most important findings of this study is that the number of the generated designs can act as a misleading confounder in quality analysis – an issue we term the 'size trap'. Such trap has significant implications: similarity and diversity metrics must be compared across libraries of consistent sizes. We also advocate for reporting these metrics

for more than 10^5 designs. To address the computational challenges of diversity assessment of large libraries, we introduce the number of substructures as a fast and reliable metric.

This study also bridges knowledge gaps and highlights barriers in the quest to 'tame the jungle' of generative drug discovery. By strengthening the connections between drug discovery and natural language processing^[60], we emphasise the usefulness of design likelihoods to select molecules for prospective studies, remove "recurring hallucinations", and rationalize the exploration-exploitation trade-off. Additionally, we uncover key differences between the two fields in the generation phase, revealing characteristic properties of molecule generation. In this context, we recommend temperature sampling as an effective strategy to navigate the chemical space with generative deep learning approaches.

Drug discovery is inherently a multi-objective endeavor,

Table 1. *Traps, treasures, and ways out.* Summary of identified the pitfalls, robust tools, and guidelines proposed in this study. These considerations were divided based on the evaluation stage they pertain to.

Stage	Trap	Treasure	Way Out
Library similarity	Library size. Metrics like FCD and FDD are dependent on library size, and decrease with increasing number of designs.	FCD. FCD plateaus for more than 10,000 designs, making it suitable even with few reference bioactive molecules.	Evaluating large libraries. Report FCD values for more than 10,000 designs, and FDD values for more than 1000 designs.
Internal diversity	Uniqueness artifacts. Uniqueness decreases as library size increases and can rank models differently at different scales.	Number of substructures. The number of substructures is a compute-efficient and size-invariant measure of internal diversity.	Size-invariant metrics. The number of clusters and the number of substructures provide consistent rankings and highlight model differences when large library sizes ($\geq 10^5$) are considered.
Molecule selection	Excessive likelihood. Highly-likely designs favor exploitation (similarity to known actives) but sacrifice novelty and diversity, limiting chemical space exploration.	Likelihood binning. Likelihood deciles enable systematic library analysis and trade-off tuning for exploration vs. exploitation, tailored to study goals.	Likelihood tuning. Select likelihood deciles for specific objectives: favor exploration for hit identification or exploitation for lead optimization.
	Count trap. Models over-generate simple and repetitive substructures, resulting in low-quality designs unsuitable for follow-up studies.	Likelihood binning. Likelihood-based scoring uncovers repetitive, low-value generations and connects generative drug discovery to NLP phenomena like “recurring hallucinations”.	Likelihood-guided filtering. Use likelihood and structural evaluations jointly to identify and deprioritize frequent but poor-quality designs in library analysis.
Molecule generation	Token filtering. Considering a small token subset during molecule sampling (via top-k or top-p sampling) cause mode collapse (repetitive, low-diversity designs).	Temperature sampling. Temperature sampling is the most effective strategy to control diversity and balance novelty vs. validity.	Varying T values. Controlling diversity through token subsets is ineffective due to the unique behavior of molecule sampling. Temperature sampling should be used, with varying T to tune lead optimization vs. diversity-focused exploration.

making the definition and measurement of design quality a persistent challenge. However, we expect that the insights and connections uncovered in this study will provide a solid foundation for making an *informed progress* towards pushing the current boundaries of generative drug discovery.

Methods

Datasets

Pre-training set. 2,372,675 SMILES strings were obtained from ChEMBL v33^[44]. Salts were removed and molecules composed only of C, H, O, N, S, P, F, Cl, Br, I atoms were retained. The SMILES strings of the remaining compounds were sanitized, canonicalized, and the charge and stereochemistry annotations were removed. SMILES strings longer than 80 tokens were dropped. The final set consisting of 1,584,858 molecules was randomly divided into

training ($n = 1,500,000$), validation ($n = 40,000$), and test splits ($n = 44,858$).

Fine-tuning sets. The fine-tuning datasets were curated from ExCAPE-DB^[45]. The targets Dopamine Receptor D3 (DRD3), peptidyl-prolyl cis/trans isomerase (PIN1), and Vitamin D Receptor (VDR) were selected. The bioactive molecules available in the pre-training set were excluded, and the remaining molecules underwent the same pre-processing steps as described above. 320 training, 128 validation, and 128 test molecules were randomly sampled among the pre-processed strings. Random sampling was repeated five times, obtaining five fine-tuning sets per protein target.

Model training

A hyperparameter search was performed for model pre-training. 100 random hyperparameter combinations were sampled for each model (from a grid of 500, 405, 960 possible combinations for LSTM, S4, and GPT, respectively, Table S1). With all trained models, 8192 designs were generated and the hyperparameter combination whose designs yielded the highest novelty was chosen for follow-up fine-tuning. Early stopping on validation loss (cross-entropy) was used with a patience of five epochs for pre-training and three for fine-tuning (with tolerance of 10^{-5}).

Molecule sampling

Temperature sampling. Temperature sampling applies a smoothing parameter, temperature (T), to the next token logits predicted by a model. The sampling probability of each token t (p_t) is computed as:

$$p_t = \frac{\exp(y_t/T)}{\sum_t \exp(y_t/T)}, \quad (1)$$

where T is the temperature parameter and y_t is the logit output by the model for the token t . Increasing the temperature value increases the uniformity of the distribution (uniform distribution for $T \rightarrow \infty$), while decreasing the temperature value decreases the randomness (Dirac distribution for $T \rightarrow 0$). When $T = 1$, the so-called multinomial sampling (where the probability of generating each token is determined by the model output) is performed. We experimented with 0.5, 0.75, 1.0, 1.25, 1.5, 1.75, and 2.0 as T values in this study.

Top- k sampling. Top- k sampling^[57] samples the next token from the most likely k tokens. Increasing the k values to the number of tokens in the vocabulary makes it equivalent to temperature sampling. Using $k = 1$ is equivalent to greedy sampling, i.e., sampling the most likely token at each step. We experimented with values of k equal to 3, 5, 10, 15, 20, 25, and 30 (with a vocabulary size equal to 33).

Top- p sampling. Top- p sampling^[57] (also known as nucleus sampling) samples the next token from the minimum cardinality set whose summed probabilities exceed the threshold p ($0 \leq p \leq 1$). Decreasing the value of p includes fewer tokens in the selection and helps to avoid degenerate outputs, while trading diversity off^[57]. Top- p sampling approximates greedy sampling as $p \rightarrow 0$ and is equivalent to temperature sampling when $p = 1.0$. In this study, we experimented with values of p equal to 0.5, 0.6, 0.7, 0.8, 0.9, 0.925, 0.950, and 0.975.

Sampling strategy. From each target (3x), each data split (5x), and each model architecture (3x), we generated 1,000,000 SMILES strings per sampling strategy and sam-

pling parameter (T , k and p , 22 values tested in total). This resulted in a total of $3 \times 5 \times 3 \times 22 \times 10^6 = 990,000,000 = 9.9 \times 10^8 \approx 10^9$ molecules that were designed and evaluated in this study.

Evaluation metrics

Syntactic Score. Validity was computed as the fraction of the designed SMILES strings corresponding to ‘chemically valid’ molecules. Uniqueness was computed as the percentage of distinct canonical SMILES strings among the valid ones. Novelty was computed as the fraction of valid and unique designs that were not present in either the pre-training and fine-tuning sets.

Similarity.

- The Fréchet ChemNet Distance (FCD)^[46] was computed using the `fcd` library released by the authors.
- The Fréchet distance^[48] between molecular descriptor distributions (FDD) was computed using the following descriptors: octanol-water partitioning coefficient^[61], molecular weight, number of hydrogen bond donors, number of rings, and topological surface area. Molecular descriptors were computed via `rdkit`, and min-max normalized to global maximum and minimum values before distance calculation.
- The substructure similarity was computed via Tanimoto similarity on extended connectivity fingerprints (ECFPs)^[50]. ECFPs were computed with `rdkit` (`fpSize=2048`, and `radius=2`).

Internal diversity The number of clusters was computed by using the sphere exclusion algorithm implemented in the `LeaderPicker` module of `rdkit`. We used a distance threshold of 0.6, using the Tanimoto similarity on ECFPs. This is equivalent to computing #Circles metric^[49]. The number of substructures was calculated by counting the number of unique fingerprint keys identified by the Morgan algorithm (`rdkit`, `radius=2`).

Design likelihood

Likelihood of a design d (\mathcal{L}_d) was computed by multiplying the sampling probability p_t of each SMILES token t :

$$\mathcal{L}_d = \prod_t p_t \quad (2)$$

where t runs over the tokens in the designed sequence. The log-sum-exp trick was used to mitigate numerical instabilities.

Data availability

The data used and generated in our study will be available on Zenodo upon paper acceptance and on GitHub at the following URL: <https://github.com/molML/jungle-of-generative-drug-discovery>.

Code availability

The Python code to replicate our study will be available on Zenodo upon paper acceptance and on GitHub at the following URL: <https://github.com/molML/jungle-of-generative-drug-discovery>.

Author Contributions

Conceptualization: all authors. Data curation: R.Ö. Formal analysis: all authors. Investigation: all authors. Methodology: all authors. Software: R.Ö. Visualization: R.Ö. Writing – original draft: R.Ö. Writing – review and editing: all authors.

Acknowledgements

This research was co-funded by the European Union (ERC, ReMINDER, 101077879). Views and opinions expressed are however those of the author(s) only and do not necessarily reflect those of the European Union or the European Research Council. Neither the European Union nor the granting authority can be held responsible for them. The authors also acknowledge support from the Irene Curie Fellowship, the Centre for Living Technologies. The authors thank Selen Parlar and Helena Brinkmann for their feedback on the manuscript.

Competing interests

The authors declare no competing interests.

References

- [1] O. J. Wouters, M. McKee, and J. Luyten, “Estimated research and development investment needed to bring a new medicine to market, 2009–2018,” *Jama*, vol. 323, no. 9, pp. 844–853, 2020.
- [2] J. A. DiMasi, H. G. Grabowski, and R. W. Hansen, “Innovation in the pharmaceutical industry: new estimates of r&d costs,” *Journal of health economics*, vol. 47, pp. 20–33, 2016.
- [3] R. S. Bohacek, C. McMartin, and W. C. Guida, “The art and practice of structure-based drug design: a molecular modeling perspective,” *Medicinal research reviews*, vol. 16, no. 1, pp. 3–50, 1996.
- [4] J. M. Stokes, K. Yang, K. Swanson, W. Jin, A. Cubillos-Ruiz, N. M. Donghia, C. R. MacNair, S. French, L. A. Carfrae, Z. Bloom-Ackermann, *et al.*, “A deep learning approach to antibiotic discovery,” *Cell*, vol. 180, no. 4, pp. 688–702, 2020.
- [5] G. Liu, D. B. Catacutan, K. Rathod, K. Swanson, W. Jin, J. C. Mohammed, A. Chiappino-Pepe, S. A. Syed, M. Fragis, K. Rachwalski, *et al.*, “Deep learning-guided discovery of an antibiotic targeting *acinetobacter baumannii*,” *Nature Chemical Biology*, vol. 19, no. 11, pp. 1342–1350, 2023.
- [6] F. Wong, E. J. Zheng, J. A. Valeri, N. M. Donghia, M. N. Anahtar, S. Omori, A. Li, A. Cubillos-Ruiz, A. Krishnan, W. Jin, *et al.*, “Discovery of a structural class of antibiotics with explainable deep learning,” *Nature*, vol. 626, no. 7997, pp. 177–185, 2024.
- [7] W. J. Godinez, E. J. Ma, A. T. Chao, L. Pei, P. Skewes-Cox, S. M. Canham, J. L. Jenkins, J. M. Young, E. J. Martin, and W. A. Guiguemde, “Design of potent antimalarials with generative chemistry,” *Nature Machine Intelligence*, vol. 4, no. 2, pp. 180–186, 2022.
- [8] F. Wan, D. Kontogiorgos-Heintz, and C. de la Fuente-Nunez, “Deep generative models for peptide design,” *Digital Discovery*, vol. 1, no. 3, pp. 195–208, 2022.
- [9] M. Moret, I. Pachon Angona, L. Cotos, S. Yan, K. Atz, C. Brunner, M. Baumgartner, F. Grisoni, and G. Schneider, “Leveraging molecular structure and bioactivity with chemical language models for de novo drug design,” *Nature Communications*, vol. 14, no. 1, p. 114, 2023.
- [10] Y. Li, L. Zhang, Y. Wang, J. Zou, R. Yang, X. Luo, C. Wu, W. Yang, C. Tian, H. Xu, *et al.*, “Generative deep learning enables the discovery of a potent and selective ripk1 inhibitor,” *Nature Communications*, vol. 13, no. 1, p. 6891, 2022.
- [11] L. Isigkeit, T. Hörmann, E. Schallmayer, K. Scholz, F. F. Lillich, J. H. Ehrler, B. Hufnagel, J. Büchner, J. A. Marschner, J. Pabel, *et al.*, “Automated design of multi-target ligands by generative deep learning,” *Nature Communications*, vol. 15, no. 1, p. 7946, 2024.
- [12] Y. Xia, K. Wu, P. Deng, R. Liu, Y. Zhang, H. Guo, Y. Cui, Q. Pei, L. Wu, S. Xie, *et al.*, “Target-aware molecule generation for drug design using a chemical language model,” *bioRxiv*, pp. 2024–01, 2024.
- [13] Y. Bian and X.-Q. Xie, “Generative chemistry: drug discovery with deep learning generative models,” *Journal of Molecular Modeling*, vol. 27, pp. 1–18, 2021.

- [14] A. Gangwal and A. Lavecchia, "Unlocking the potential of generative ai in drug discovery," *Drug Discovery Today*, p. 103992, 2024.
- [15] Y. Cheng, Y. Gong, Y. Liu, B. Song, and Q. Zou, "Molecular design in drug discovery: a comprehensive review of deep generative models," *Briefings in bioinformatics*, vol. 22, no. 6, p. bbab344, 2021.
- [16] A. Volkamer, S. Riniker, E. Nittinger, J. Lanini, F. Grisoni, E. Evertsson, R. Rodríguez-Pérez, and N. Schneider, "Machine learning for small molecule drug discovery in academia and industry," *Artificial Intelligence in the Life Sciences*, vol. 3, p. 100056, 2023.
- [17] D. B. Catacutan, J. Alexander, A. Arnold, and J. M. Stokes, "Machine learning in preclinical drug discovery," *Nature Chemical Biology*, vol. 20, no. 8, pp. 960–973, 2024.
- [18] W. Yuan, D. Jiang, D. K. Nambiar, L. P. Liew, M. P. Hay, J. Bloomstein, P. Lu, B. Turner, Q.-T. Le, R. Tibshirani, *et al.*, "Chemical space mimicry for drug discovery," *Journal of chemical information and modeling*, vol. 57, no. 4, pp. 875–882, 2017.
- [19] D. Merk, L. Friedrich, F. Grisoni, and G. Schneider, "De novo design of bioactive small molecules by artificial intelligence," *Molecular informatics*, vol. 37, no. 1-2, p. 1700153, 2018.
- [20] F. Grisoni, B. J. Huisman, A. L. Button, M. Moret, K. Atz, D. Merk, and G. Schneider, "Combining generative artificial intelligence and on-chip synthesis for de novo drug design," *Science Advances*, vol. 7, no. 24, p. eabg3338, 2021.
- [21] M. Ballarotto, S. Willems, T. Stiller, F. Nawa, J. A. Marschner, F. Grisoni, and D. Merk, "De novo design of nurr1 agonists via fragment-augmented generative deep learning in low-data regime," *Journal of Medicinal Chemistry*, 2023.
- [22] M. H. Segler, T. Kogej, C. Tyrchan, and M. P. Waller, "Generating focused molecule libraries for drug discovery with recurrent neural networks," *ACS central science*, vol. 4, no. 1, pp. 120–131, 2018.
- [23] R. Gómez-Bombarelli, J. N. Wei, D. Duvenaud, J. M. Hernández-Lobato, B. Sánchez-Lengeling, D. Sheberla, J. Aguilera-Iparraguirre, T. D. Hirzel, R. P. Adams, and A. Aspuru-Guzik, "Automatic chemical design using a data-driven continuous representation of molecules," *ACS central science*, vol. 4, no. 2, pp. 268–276, 2018.
- [24] T. Sousa, J. Correia, V. Pereira, and M. Rocha, "Generative deep learning for targeted compound design," *Journal of chemical information and modeling*, vol. 61, no. 11, pp. 5343–5361, 2021.
- [25] F. Grisoni, "Chemical language models for de novo drug design: Challenges and opportunities," *Current Opinion in Structural Biology*, vol. 79, p. 102527, 2023.
- [26] R. Özçelik, S. de Ruiter, E. Criscuolo, and F. Grisoni, "Chemical language modeling with structured state space sequence models," *Nature Communications*, vol. 15, no. 1, p. 6176, 2024.
- [27] A. Gupta, A. T. Müller, B. J. Huisman, J. A. Fuchs, P. Schneider, and G. Schneider, "Generative recurrent networks for de novo drug design," *Molecular informatics*, vol. 37, no. 1-2, p. 1700111, 2018.
- [28] D. Polykovskiy, A. Zhebrak, B. Sanchez-Lengeling, S. Golovanov, O. Tatanov, S. Belyaev, R. Kurbanov, A. Artamonov, V. Aladinskiy, M. Veselov, *et al.*, "Molecular sets (moses): a benchmarking platform for molecular generation models," *Frontiers in pharmacology*, vol. 11, p. 565644, 2020.
- [29] N. Brown, M. Fiscato, M. H. Segler, and A. C. Vaucher, "Guacamol: benchmarking models for de novo molecular design," *Journal of chemical information and modeling*, vol. 59, no. 3, pp. 1096–1108, 2019.
- [30] J. Arús-Pous, T. Blaschke, S. Ulander, J.-L. Reymond, H. Chen, and O. Engkvist, "Exploring the gdb-13 chemical space using deep generative models," *Journal of cheminformatics*, vol. 11, pp. 1–14, 2019.
- [31] D. Nie, H. Zhao, O. Zhang, G. Weng, H. Zhang, J. Jin, H. Lin, Y. Huang, L. Liu, D. Li, *et al.*, "Durian: A comprehensive benchmark for structure-based 3d molecular generation," *Journal of Chemical Information and Modeling*, 2024.
- [32] P. Renz, D. Van Rompaey, J. K. Wegner, S. Hochreiter, and G. Klambauer, "On failure modes in molecule generation and optimization," *Drug Discovery Today: Technologies*, vol. 32, pp. 55–63, 2019.
- [33] A. Bender, N. Schneider, M. Segler, W. Patrick Walters, O. Engkvist, and T. Rodrigues, "Evaluation guidelines for machine learning tools in the chemical sciences," *Nature Reviews Chemistry*, vol. 6, no. 6, pp. 428–442, 2022.
- [34] D. D. Martinelli, "Generative machine learning for de novo drug discovery: A systematic review," *Computers in Biology and Medicine*, vol. 145, p. 105403, 2022.

- [35] M. A. Skinnider, R. G. Stacey, D. S. Wishart, and L. J. Foster, "Chemical language models enable navigation in sparsely populated chemical space," *Nature Machine Intelligence*, vol. 3, no. 9, pp. 759–770, 2021.
- [36] D. Flam-Shepherd, K. Zhu, and A. Aspuru-Guzik, "Language models can learn complex molecular distributions," *Nature Communications*, vol. 13, no. 1, p. 3293, 2022.
- [37] D. Weininger, "Smiles, a chemical language and information system. 1. introduction to methodology and encoding rules," *Journal of chemical information and computer sciences*, vol. 28, no. 1, pp. 31–36, 1988.
- [38] M. Krenn, Q. Ai, S. Barthel, N. Carson, A. Frei, N. C. Frey, P. Friederich, T. Gaudin, A. A. Gayle, K. M. Jablonka, *et al.*, "Selfies and the future of molecular string representations," *Patterns*, vol. 3, no. 10, 2022.
- [39] S. Hochreiter and J. Schmidhuber, "Long short-term memory," *Neural computation*, vol. 9, no. 8, pp. 1735–1780, 1997.
- [40] A. Radford, J. Wu, R. Child, D. Luan, D. Amodei, I. Sutskever, *et al.*, "Language models are unsupervised multitask learners," *OpenAI blog*, vol. 1, no. 8, p. 9, 2019.
- [41] V. Bagal, R. Aggarwal, P. Vinod, and U. D. Priyakumar, "Molgppt: molecular generation using a transformer-decoder model," *Journal of Chemical Information and Modeling*, vol. 62, no. 9, pp. 2064–2076, 2021.
- [42] D. Bahdanau, K. H. Cho, and Y. Bengio, "Neural machine translation by jointly learning to align and translate," in *3rd International Conference on Learning Representations, ICLR 2015*, 2015.
- [43] A. Gu, K. Goel, and C. Ré, "Efficiently modeling long sequences with structured state spaces," in *The International Conference on Learning Representations (ICLR)*, 2022.
- [44] A. Gaulton, A. Hersey, M. Nowotka, A. P. Bento, J. Chambers, D. Mendez, P. Mutowo, F. Atkinson, L. J. Bellis, E. Cibrián-Uhalte, *et al.*, "The chembl database in 2017," *Nucleic acids research*, vol. 45, no. D1, pp. D945–D954, 2017.
- [45] J. Sun, N. Jeliaskova, V. Chupakhin, J.-F. Golib-Dzib, O. Engkvist, L. Carlsson, J. Wegner, H. Ceulemans, I. Georgiev, V. Jeliaskov, *et al.*, "Excapedb: an integrated large scale dataset facilitating big data analysis in chemogenomics," *Journal of cheminformatics*, vol. 9, pp. 1–9, 2017.
- [46] K. Preuer, P. Renz, T. Unterthiner, S. Hochreiter, and G. Klambauer, "Fréchet chemnet distance: a metric for generative models for molecules in drug discovery," *Journal of chemical information and modeling*, vol. 58, no. 9, pp. 1736–1741, 2018.
- [47] A. Mayr, G. Klambauer, T. Unterthiner, M. Steijaert, J. K. Wegner, H. Ceulemans, D.-A. Clevert, and S. Hochreiter, "Large-scale comparison of machine learning methods for drug target prediction on chembl," *Chemical science*, vol. 9, no. 24, pp. 5441–5451, 2018.
- [48] M. Fréchet, "Sur la distance de deux lois de probabilité," in *Annales de l'ISUP*, vol. 6, pp. 183–198, 1957.
- [49] Y. Xie, Z. Xu, J. Ma, and Q. Mei, "How much space has been explored? measuring the chemical space covered by databases and machine-generated molecules," in *The Eleventh International Conference on Learning Representations*, 2023.
- [50] D. Rogers and M. Hahn, "Extended-connectivity fingerprints," *Journal of chemical information and modeling*, vol. 50, no. 5, pp. 742–754, 2010.
- [51] D. P. Kingma and M. Welling, "Auto-encoding variational bayes," 2022.
- [52] G. Papamakarios, E. Nalisnick, D. J. Rezende, S. Mohamed, and B. Lakshminarayanan, "Normalizing flows for probabilistic modeling and inference," *Journal of Machine Learning Research*, vol. 22, no. 57, pp. 1–64, 2021.
- [53] P. Laban, C.-S. Wu, W. Liu, and C. Xiong, "Near-negative distinction: Giving a second life to human evaluation datasets," in *Proceedings of the 2022 Conference on Empirical Methods in Natural Language Processing*, pp. 2094–2108, 2022.
- [54] M. Moret, F. Grisoni, P. Katzberger, and G. Schneider, "Perplexity-based molecule ranking and bias estimation of chemical language models," *Journal of chemical information and modeling*, vol. 62, no. 5, pp. 1199–1206, 2022.
- [55] G. W. Bemis and M. A. Murcko, "The properties of known drugs. 1. molecular frameworks," *Journal of medicinal chemistry*, vol. 39, no. 15, pp. 2887–2893, 1996.
- [56] L. Huang, W. Yu, W. Ma, W. Zhong, Z. Feng, H. Wang, Q. Chen, W. Peng, X. Feng, B. Qin, *et al.*, "A survey on hallucination in large language models: Principles, taxonomy, challenges, and open questions," *arXiv preprint arXiv:2311.05232*, 2023.

- [57] A. Holtzman, J. Buys, L. Du, M. Forbes, and Y. Choi, “The curious case of neural text degeneration,” *arXiv preprint arXiv:1904.09751*, 2019.
- [58] A. Fan, M. Lewis, and Y. Dauphin, “Hierarchical neural story generation,” in *Proceedings of the 56th Annual Meeting of the Association for Computational Linguistics (Volume 1: Long Papers)*, Association for Computational Linguistics, 2018.
- [59] H. Zhang, D. Duckworth, D. Ippolito, and A. Neelakantan, “Trading off diversity and quality in natural language generation,” *arXiv preprint arXiv:2004.10450*, 2020.
- [60] H. Öztürk, A. Özgür, P. Schwaller, T. Laino, and E. Ozkirimli, “Exploring chemical space using natural language processing methodologies for drug discovery,” *Drug Discovery Today*, vol. 25, no. 4, pp. 689–705, 2020.
- [61] S. A. Wildman and G. M. Crippen, “Prediction of physicochemical parameters by atomic contributions,” *Journal of chemical information and computer sciences*, vol. 39, no. 5, pp. 868–873, 1999.
- [62] P. Ertl and A. Schuffenhauer, “Estimation of synthetic accessibility score of drug-like molecules based on molecular complexity and fragment contributions,” *Journal of cheminformatics*, vol. 1, pp. 1–11, 2009.

Supporting Information

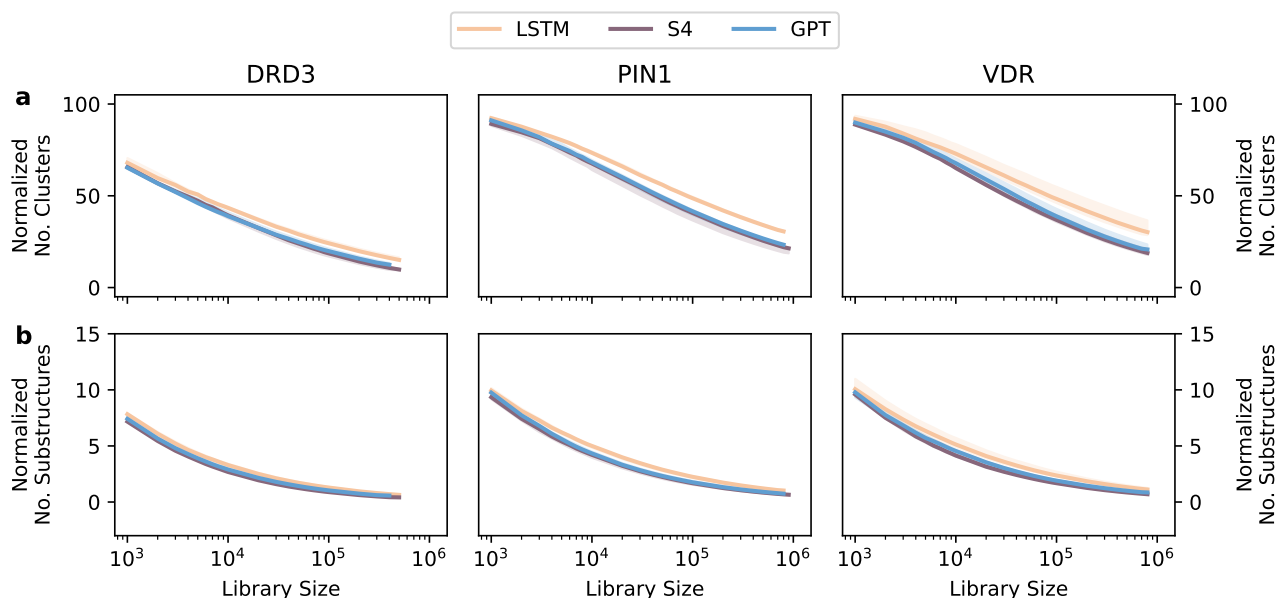
The Jungle of Generative Drug Discovery:
Traps, Treasures, and Ways OutRıza Özçelik^{1,2}, Francesca Grisoni^{1,2,*}¹Institute for Complex Molecular Systems and Dept. Biomedical Engineering, Eindhoven University of Technology, Eindhoven, Netherlands.²Centre for Living Technologies, Alliance TU/e, WUR, UU, UMC Utrecht, Netherlands.

Figure S1. Diversity metrics divided by library size. Number of substructures and clusters are computed in increasing library sizes, and divided by the number of molecules in the library. The same experimental and visualization setups are used as Figure 2.

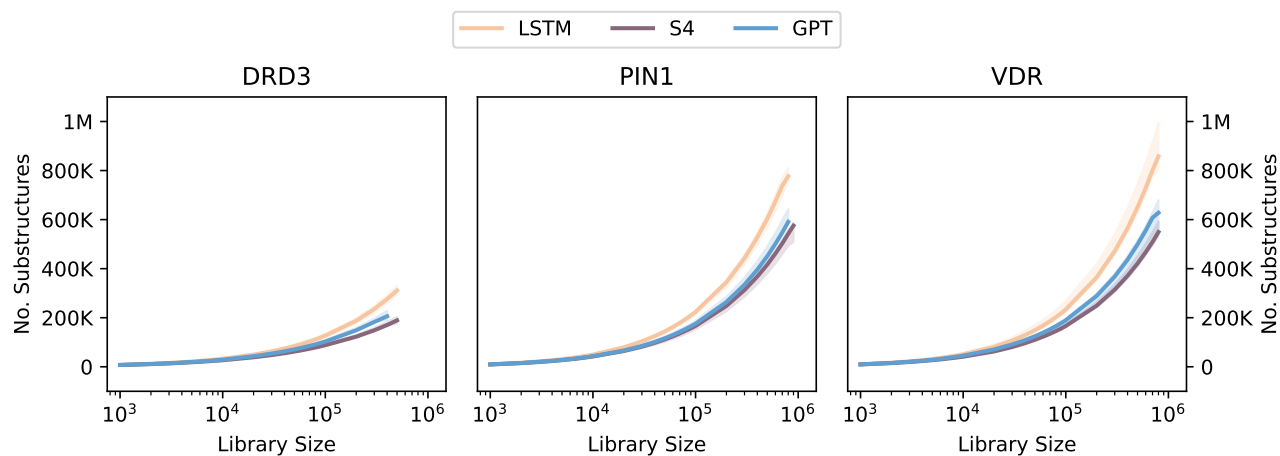


Figure S2. Effect of synthesizability filtering on internal diversity. Synthetic accessibility of the designs are computed^[62] and the generations with a score above 6 are filtered out^[62]. Number of substructures is computed with the remaining compounds. The same experimental and visualization setups are used as Figure 2.

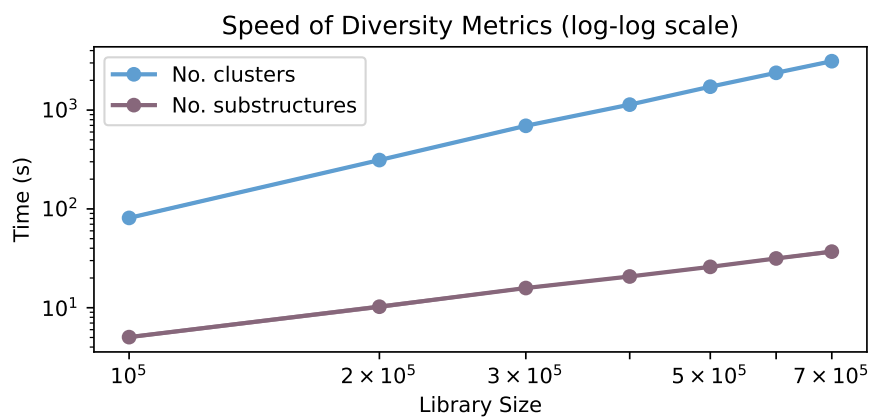


Figure S3. Speed comparison of internal diversity metrics. Number of clusters and substructures are computed in increasing library sizes, and number of seconds per computation is measured. Each computation is repeated 10 times and the average time passed is reported in log-log scale.

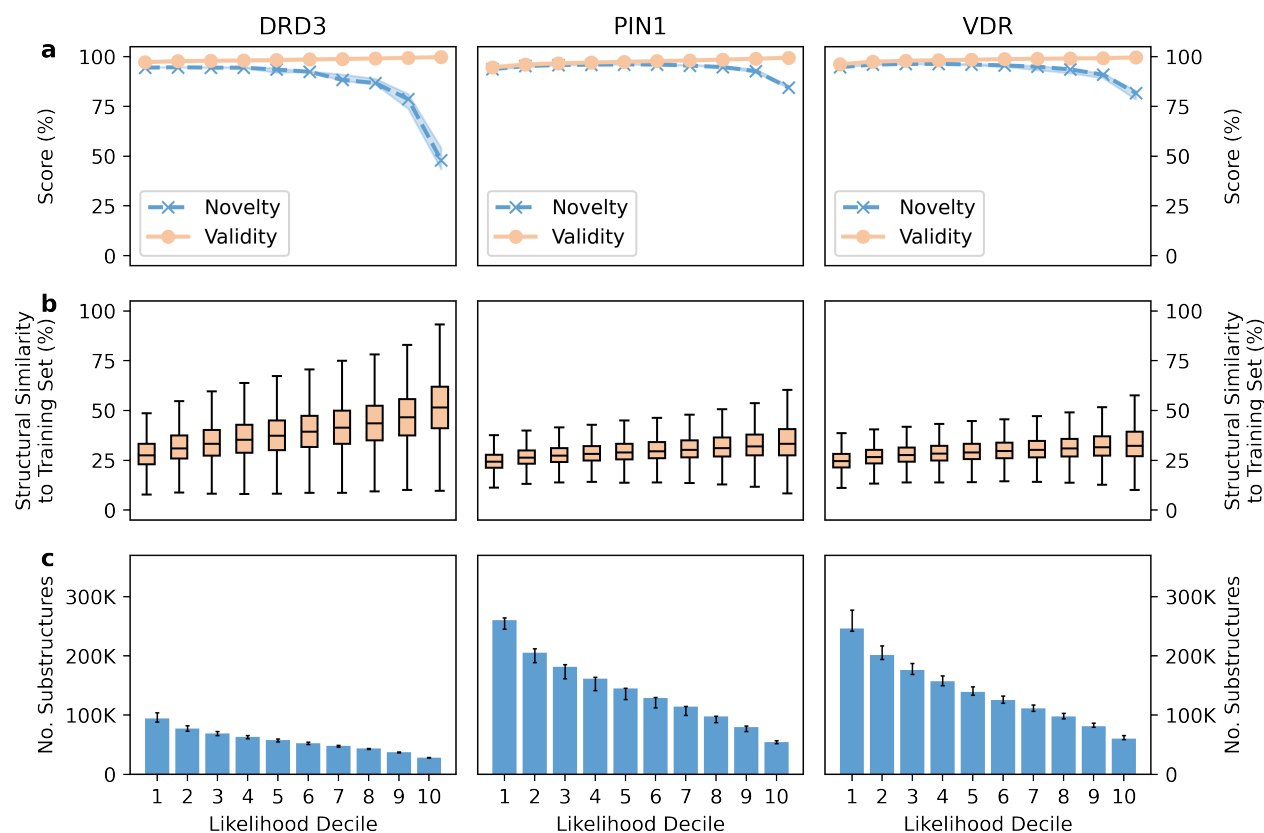


Figure S4. Navigating the design libraries of S4 architecture. The designs of fine-tuned S4 models are divided into smaller libraries of increasing design likelihoods. Validity (a), novelty (a), structural similarity to the training set (b), and internal diversity (c) are visualized as in Figure 3.

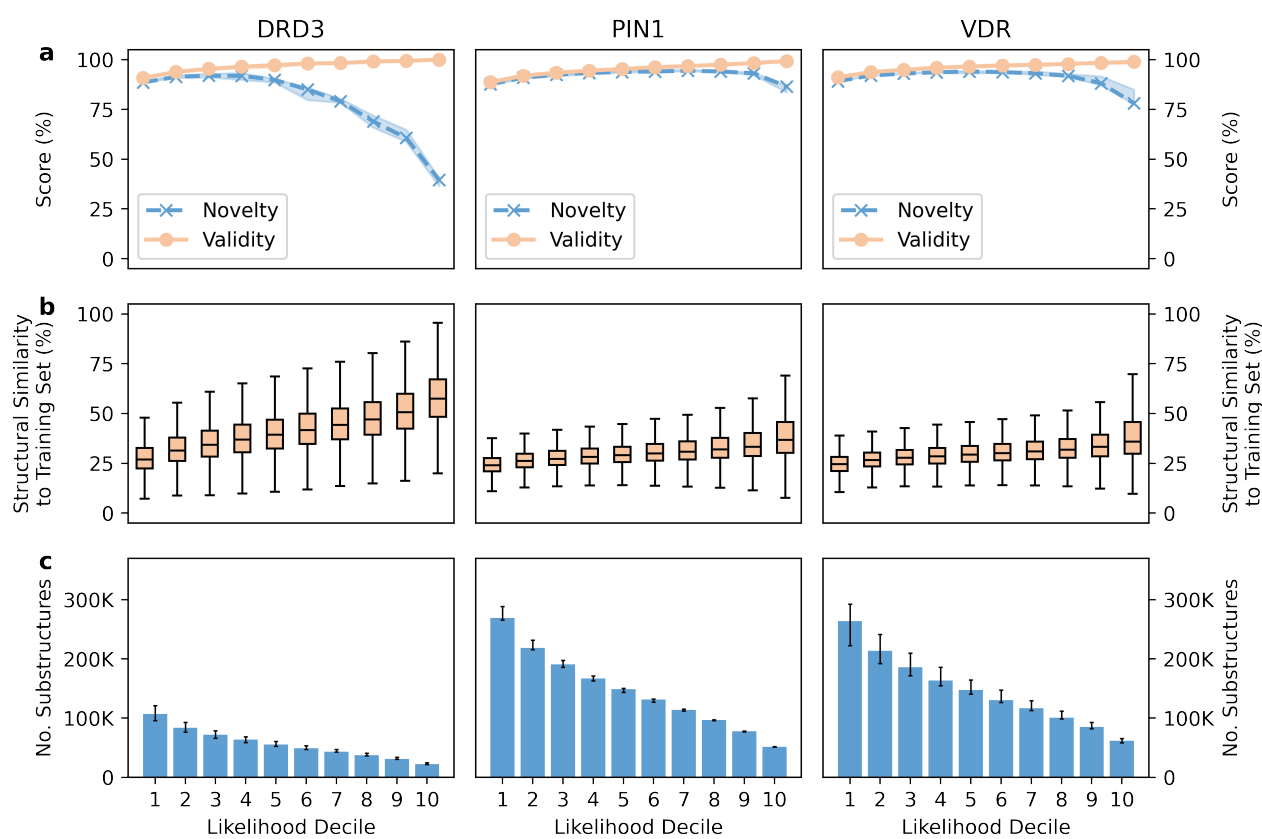


Figure S5. Navigating the design libraries of GPT architecture. The designs of fine-tuned GPT models are divided into smaller libraries of increasing design likelihoods. Validity (**a**), novelty (**a**), structural similarity to the training set (**b**), and internal diversity (**c**) are visualized as in Figure 3.

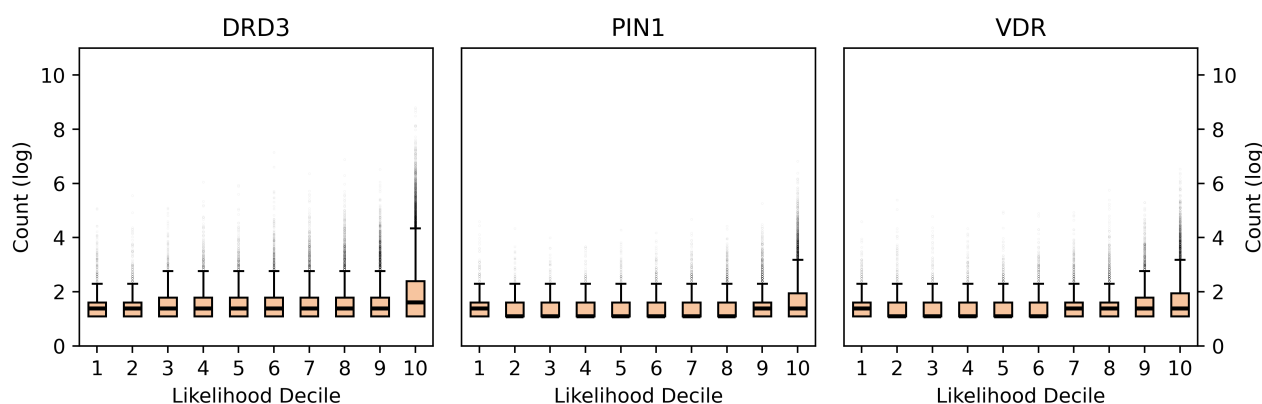


Figure S6. Design likelihood and frequency. The repeated designs of the LSTM models per target are divided into increasing likelihood bins and their log-frequencies are visualized as a box plot.

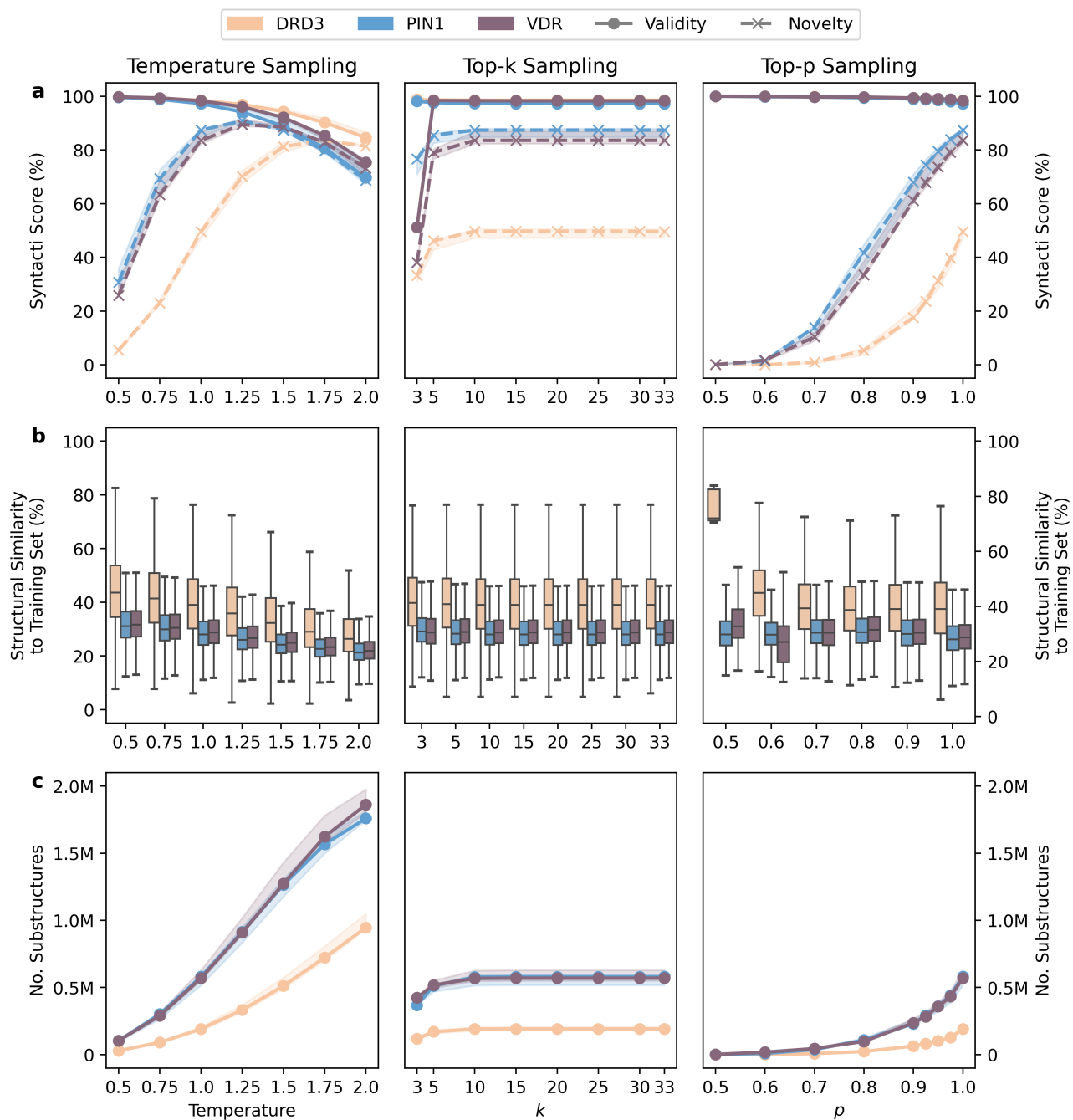


Figure S7. Benchmarking molecule sampling strategies with S4. Temperature, top-k, and top-p sampling are used to generate molecules with the fine-tuned S4 models, in increasing parameters. Syntactic quality (a), structural similarity to the fine-tuning set (b), and internal diversity (c) are visualized. Same sampling and plotting parameters are used as Figure 5.

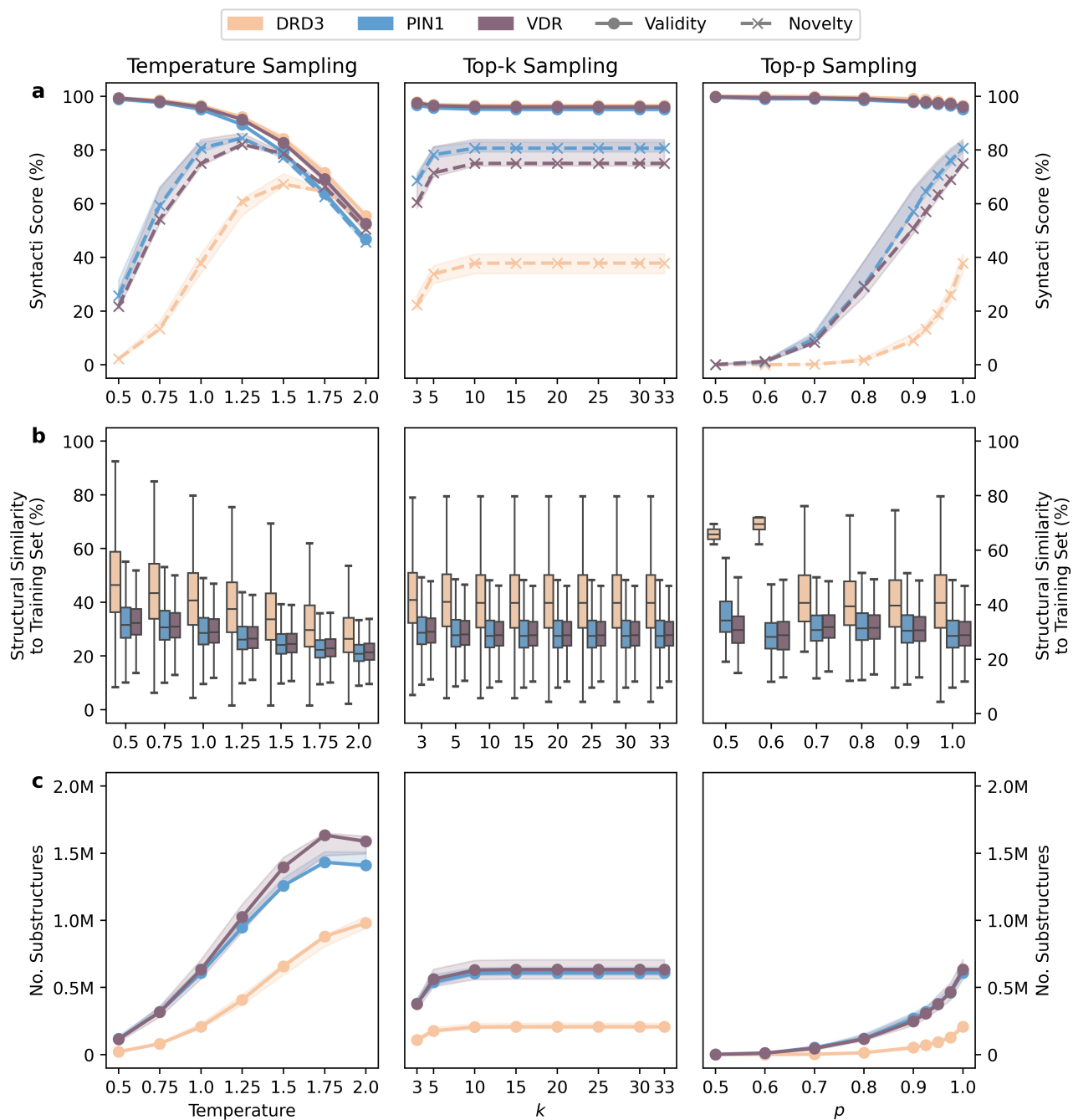


Figure S8. Benchmarking molecule sampling strategies with GPT. Temperature, top- k , and top- p sampling are used to generate molecules with the fine-tuned S4 models, in increasing parameters. Syntactic quality (a), structural similarity to the fine-tuning set (b), and internal diversity (c) are visualized. Same sampling and plotting parameters are used as Figure 5.

Table S1. Values used for hyperparameter optimization.

Architecture	Hyperparameter	Values
LSTM	Number of Layers	1, 2, 4, 6, 8
	Model dimension	256, 512, 1024, 2048
	Dropout	0.0, 0.1, 0.15, 0.2, 0.25
S4	Number of Layers	4, 6, 8
	Model dimension	256, 512, 1024
	Hidden stat dim.	128, 256, 512
	Number of SSMs	1
	Dropout	0.0, 0.1, 0.2
GPT	Number of Layers	2, 4, 6, 8
	Model dimension	128, 256, 512, 1024
	Number of Attention Heads	2, 4, 8, 16
	Dropout	0.0, 0.1, 0.2
All	Sequence length	82
	Learning rate	1e-4, 5e-4, 1e-3, 5e-3, 1e-2
	Number of max epochs	1000
	Batch size	8192